Published in final edited form as:

Nat Microbiol. 2018 December ; 3(12): 1346–1353. doi:10.1038/s41564-018-0253-0.

Anaerobic nitrate reduction divergently governs population expansion of the enteropathogen *Vibrio cholerae.*

Emilio Bueno[1], **Brandon Sit**[2,3], **Matthew K. Waldor**[2,3,4], and **Felipe Cava**[1]

[1]Laboratory for Molecular Infection Medicine Sweden, Department of Molecular Biology, Umeå Centre for Microbial Research, Umeå University, Umeå SE-90187, Sweden

[2]Department of Microbiology and Immunobiology, Harvard Medical School, Boston, MA 02115

[3]Division of Infectious Diseases, Brigham & Women's Hospital, Boston, MA 02115

[4]Howard Hughes Medical Institute, Boston, MA 02115

Abstract

To survive and proliferate in the absence of oxygen, many enteric pathogens can undergo anaerobic respiration within the host by using nitrate (NO_3^-) as electron acceptor [1,2]. In these bacteria, NO_3^- is typically reduced by a nitrate reductase to nitrite (NO_2^-), a toxic intermediate that is further reduced by a nitrite reductase[3]. However, *Vibrio cholerae,* the intestinal pathogen that causes cholera, lacks a nitrite reductase, leading to NO_2^- accumulation during nitrate reduction[4]. Thus, *V. cholerae* is thought to be unable to undergo NO_3^--dependent anaerobic respiration[4]. Here, we show that during hypoxic growth, NO_3^- reduction in *V. cholerae* divergently impacts bacterial fitness in a manner dependent on environmental pH. Remarkably, in alkaline conditions, *V. cholerae* can reduce NO_3^- to support population growth. Conversely, in acidic conditions, accumulation of NO_2^- from NO_3^- reduction simultaneously limits population expansion and preserves cell viability by lowering fermentative acid production. Interestingly, other bacterial species such as *Salmonella typhimurium,* enterohemorrhagic *Escherichia coli* (EHEC) and *Citrobacter rodentium* also reproduced this pH-dependent response suggesting that this mechanism might be conserved within enteric pathogens. Our findings explain how a bacterial pathogen can use a single redox reaction to divergently regulate population expansion depending on fluctuating environmental pH.

Keywords

Nitrate respiration; nitrite; pH; *Vibrio cholerae*; enteropathogen; fermentation; fitness

Correspondence to: felipe.cava@molbiol.umu.se.

Authors' contribution.

E.B. performed bacterial *in vitro* experiments and analyzed the results. B.S. performed animal experiments. E.B. and F. C. were responsible for the overall study design. E.B., B.S., M. K. W. and F. C. were responsible for the writing of the manuscript.

Competing interests.

The authors declare no competing interests.

Recent studies have illuminated the role of anaerobic metabolism in regulating virulence phenotypes during pathogen growth in hypoxic (oxygen-limited) host environments, such as the intestine[5,6,7]. During hypoxia and anoxia, bacteria can either undergo fermentation or utilize an alternative electron acceptor (AEA) such as dimethyl-sulphoxide (DMSO), trimethylamine N-oxide (TMAO), and fumarate to fuel oxidative phosphorylation[8]. Intestinal pathogens such as *Salmonella typhimurium* utilize AEAs such as NO_3^- to promote population expansion during host colonization[5,9]. For NO_3^-, a nitrate reductase (Nar/Nap) uses electrons from the respiratory chain to reduce NO_3^- to NO_2^-, which is reduced by a nitrite reductase (Nrf/Nir) to NO and NH_4^+ [10]. The NO_3^- reduction pathway is largely conserved in enteric pathogens[3], however some organisms, such as the cholera pathogen *Vibrio cholerae,* do not encode all the components of the system; e.g. *V. cholerae* encodes a Nap, but not a Nrf/Nir (Fig 1a, Supplementary Table 1)[11]. *V. cholerae's* lack of a nitrite reductase introduces an apparent metabolic paradox for the pathogen: during anaerobic growth, NO_3^- reduction results in an accumulation of NO_2^-, a growth-arresting metabolite[4, 12–16]. Furthermore, since it has been suggested that this pathogen is unable to couple NO_3^- reduction to anaerobic respiratory growth[4], there is no apparent benefit for *V. cholerae* to carry out NO_3^- reduction. However, since *V. cholerae* can undergo robust anaerobic growth in the intestine, where NO_3^- is usually present[17,18] and *nap* gene expression is induced[19], we re-examined the capacity of this pathogen to undergo NO_3^--dependent respiration. In doing so, we uncovered a dual role for NO_3^- reduction by *V. cholerae* that differentially impacts pathogen fitness in environments of varying acidity.

Initially, we investigated how the presence of NO_3^- modulates *V. cholerae* growth in hypoxic conditions *in vitro.* Cultures supplemented with NO_3^- (+N) reached a lower maximum optical density (OD) at an earlier time point than those without NO_3^- (-N) (Fig. 1b). Addition of NO_3^- was also associated with rapid NO_2^- accumulation in the media (Fig. 1b). This was expected since *V. cholerae* lacks downstream nitrite reductases such as Nrf or Nir. NO_2^- concentrations and OD_{600} readings plateaued at approximately the same time (Fig. 1b, Supplementary Fig. 1), consistent with the idea that NO_2^- accumulation results in growth arrest. However, unexpectedly, when samples from these cultures were plated to quantify numbers of viable cells, there were >100-fold more colony-forming units (CFU) in +N cultures vs -N cultures at 24hr, even though the OD in the +N cultures was >2-fold lower at this time. By 48 hours, there were no detectable CFU in the -N cultures and we were unable to isolate intact genomic DNA from these cells, indicative of a loss of viability (Fig. 1b, Supplementary Fig. 2). Interestingly, when we tested other AEAs for this phenotype, none were able to maintain viability (Supplementary Fig. 3). Thus, NO_3^- specifically promotes bacterial viability while inhibiting population expansion. These disparate effects were dependent not only on the concentration of NO_3^- but also on the presence of the nitrate reductase (Nap), suggesting these phenotypes require an intact NO_3^- reduction machinery (Fig. 1a, c and Supplementary Fig. 1). Notably, addition of NO_2^- was sufficient to preserve the viability of *ΔnapA* bacteria after 2 days in hypoxic culture, a time when there were no detectable CFU in *ΔnapA* cultures that were not supplemented with NO_3^- (Fig. 1d). Thus, the reduction of NO_3^- by Nap and the concomitant accumulation of NO_2^- likely explains both the arrest of bacterial growth as well as the preservation of viability in NO_3^--replete conditions.

Monitoring the pH of -N and +N hypoxic cultures offered a clue regarding the mechanism by which NO_2^- accumulation promotes *V. cholerae* viability in these conditions. The pH of -N cultures continued to drop after ~10 hours to a final pH of 5.7, whereas at this time it plateaued at pH 6.2 in +N cultures (Fig. 2a). Notably, this is a time when *V. cholerae* growth would be arrested by Nap-dependent NO_2^- accumulation. Addition of *V. cholerae* to pre-conditioned medium (PCM) from +N cultures (pH 6.2) that had been pH-adjusted to 5.7 blocked viability, whereas adjustment of -N medium (pH 5.7) to pH 6.2 preserved viability (Fig. 2b). These observations suggested that low pH is itself a factor that leads to the loss of viability in -N cultures at 48 hours. However, cultures grown in non-fermentative medium where the pH was adjusted with hydrochloric acid (HCl) did not undergo a loss of viability (Fig. 2c), indicating that additional factor(s) in the PCM were required in conjunction with low pH to lead to cell death.

We hypothesized that this reduction in pH was due to the accumulation of mixed-acid fermentative products such as acetate, formate and lactate. When these acids were used instead of HCl to adjust the pH of the medium, there was a loss of viability like that observed in the -N cultures (Fig. 2c). Ultra-performance liquid chromatography (UPLC) analysis of culture supernatants revealed that fermentative organic acids were selectively diminished in cultures with added NO_3^- or NO_2^-, suggesting these bacteria had reduced fermentative activity, presumably due to the growth arresting effect of accumulated NO_2^- (Fig. 2d and Supplementary Fig. 5). Mixtures of organic acids used at concentrations measured in +N cultures recapitulated the effect of single acids (Fig. 2e). Together, these data indicate that the presence and accumulation of acid fermentation products during *V. cholerae* expansion leads to a loss of cell viability. However, this “fermentative acidification” is counteracted by Nap-dependent generation of nitrite, allowing *V. cholerae* to balance population expansion and the maintenance of individual cell viability in niches with little to no oxygen available. Similar results were obtained with additional enteropathogens including *S. typhimurium,* enterohemorrhagic *Escherichia coli* (EHEC) and *Citrobacter rodentium,* suggesting that this mechanism may be conserved in intestinal bacterial pathogens (Supplementary Fig. 4a-e).

Although NO_2^- is known to affect diverse cellular processes[12–16], the exact mechanism(s) by which it slows bacterial growth are not well defined. Targeted metabolomics on cultures with and without NO_3^- or NO_2^- supplementation showed that treatment with either nitrogen oxide led to similar metabolite profiles that clustered separately from nitrogen-deprived cultures (Supplementary Fig. 6a). We noted marked accumulation of early glycolytic intermediates and depletion of downstream Krebs cycle and biosynthetic products, suggesting NO_2^- had a particularly inhibitory impact on glycolysis (Fig. 2f, Supplementary Fig. 6b). We hypothesized that NO_2^--inhibition occurred at the level of phosphofructokinase (PFK), a glycolytic enzyme whose substrate, fructose-6-phosphate (F6P), was the most accumulated metabolite. Consistent with this idea, when *V. cholerae* was treated with PFK inhibitors, such as itaconic acid, cells underwent growth arrest and preserved viability (Supplementary Fig. 7a), similar to the phenotypes observed when *V. cholerae* cultures were grown with NO_3^- (Fig. 1). Furthermore, addition of NO_2^- to purified *V. cholerae* PFK inhibited its activity but not that of BsrV, an unrelated *V. cholerae* enzyme, indicating that NO_2^- can directly inhibit PFK function in a relatively specific fashion (Supplementary Fig.

7b). Thus, NO_2^- inhibition of PFK and the consequent downstream metabolic imbalances is likely an important contributor to NO_2^--mediated growth arrest. However, supplementation of cultures with metabolites from pathways downstream of PFK did not rescue growth (Supplementary Fig. 7c), suggesting that the metabolic consequences of the cellular accumulation of NO_2^- are complex and likely reflect additional factors besides inhibition of PFK. Notably, in acidic solutions, NO_2^- equilibrates to free nitrous acid, HNO_2, a strongly oxidative thiol-reactive species that can pleiotropically modify and damage proteins[13,14,16]. Collectively, these observations reveal that nitrite impedes energy-generating pathways arresting *V. cholerae* growth, which ultimately preserves cell viability.

To complement the metabolomic analyses, we undertook a genetic screen with an arrayed *V. cholerae* transposon mutant library[20] to identify mutants whose growth was not arrested by nitrite. We found that a mutant in the fermentative enzyme alcohol dehydrogenase (*adhE*) exhibited unexpected Nap-dependent enhanced growth and viability in the presence of NO_3^- (Fig. 3a, Supplementary Fig. 8, 9). The *adhE* mutant did not secrete organic acids and thus, did not acidify the media during anaerobic growth, consistent with the idea that pH reduction in the media is dependent on fermentative activity (Fig. 3a). Consequently, the viability of *ΔadhE* and *ΔadhE/napA* mutants was preserved in the absence of NO_3^- (Supplementary Fig. 8). The improved growth of *ΔadhE* in +N conditions suggests that *V. cholerae* must have some capacity to undergo NO_3^- dependent respiratory growth, contrary to a prior report[4].

To further characterize *V. cholerae*'s capacity for NO_3^- dependent anaerobic respiration, we used a rich media (LB) to avoid the effects of glucose fermentative acidification, thus minimizing the NO_2^- -induced toxicity associated with minimal media (Figs. 1 and 2). Although pH was not drastically reduced during hypoxic *V. cholerae* culture in LB (~pH 6.0), incomplete NO_3^- reduction at this pH precluded the analysis of NO_3^- -dependent growth phenotypes in these conditions (Fig. 3b, Supplementary Fig. 9b, 10a). Surprisingly, pH neutralization by addition of exogenous sodium hydroxide after 3 hours of incubation triggered complete NO_3^- reduction and concomitant growth (Fig. 3c). Consistent with this observation, *V. cholerae* grown in LB buffered at pH 8 exhibited robust Nap-dependent and NO_3^- dose-dependent population expansion and viable CFU remained recoverable for at least 48 hours (Fig. 3d, Supplementary Fig. 9c, 10b). At lower pH, the comparatively small amount of NO_2^- production is not attributable to altered Nap enzyme activity, which remained intact at pH 6 (Fig. 3e). Instead, this low pH-phenotype is likely explained by the marked impairment in the electron transport chain activity that supports NO_3^- reduction (Fig. 3f), and by a reduced cell membrane potential (Fig. 3g), which ultimately restricts the organism to a fermentative metabolic state. However, at high pH, *V. cholerae* can couple NO_3^- reduction with growth. Similar effects were observed in *S. typhimurium*, *C. rodentium* and EHEC (Supplementary Fig. 11), buttressing the idea that an elevated pH enhances the performance of the NO_3^- reduction-associated respiratory chain in diverse enteropathogens.

We addressed the positive impact of NO_3^- reduction on *V. cholerae* fitness in a variety of scenarios. Co-culture experiments in conditions where NO_2^- accumulation induces growth arrest showed that in the presence of NO_3^-, the viability of *ΔnapA* was rescued by the NO_2^- producing WT strain (Fig. 4a). Thus, in these fermentative acidic conditions, accumulated

NO_2^- can trans-complement NO_3^- reductase-deficient bacteria. Conversely, when similar co-culture assays were performed in a pH 8-buffered media to assay the impact of NO_3^- respiration, the WT strain outcompeted the *ΔnapA* mutant by nearly 100-fold within 24 hours in an NO_3^- dependent manner (Fig. 4b, Supplementary Fig. 12a, Supplementary Table 2a and 13a). Similar results were obtained in interspecies competition experiments. In low pH conditions, where *V. cholerae* NO_3^-respiration is inactive, the pathogen was outcompeted by *E. coli* K12, which retains NO_3^- respiratory activity at this pH (Fig. 4c, Supplementary Table 2a and 13b). However, in the alkaline hypoxic conditions where *V. cholerae* NO_3^- respiration is intact, the pathogen efficiently competed with *E. coli,* raising the possibility that *V. cholerae* could rely on NO_3^-respiration as a means of competition against commensal organisms. Finally, we used the streptomycin-treated adult mouse model of *V. cholerae* colonization[21] to investigate the role of nitrate respiration in colonization of a mammalian host. Streptomycin-treated mice have millimolar levels of NO_3^- in the intestine[7], providing a potential substrate for preservation of viability during fermentation or Nap-based respiration (Supplementary Fig. 1, 12a). Relative to the WT strain, the *ΔnapA* mutant was significantly outcompeted in the cecum and colon, indicating that nitrate reductase activity can enhance the capacity of the pathogen to grow in the intestine (Fig. 4d, Supplementary Fig. 12b, 14 and Supplementary Table 2b).

Our findings reveal that during anaerobic growth, *V. cholerae* can employ Nap reductase to support its fitness at both a population and individual cell level. The accumulation of nitrite, a toxic metabolite, may paradoxically preserve cell viability by slowing down metabolism in certain environmental conditions. Nitrite accumulation has been observed in numerous bacterial species[12,22–24] and in different environmental niches[18,25–27], and our results highlight the potential functional consequences for this phenomenon. Although we cannot conclude from our *in vivo* data whether nitrite at inhibitory levels accumulate in the gut, it is known that intestinal and fecal nitrate and nitrite levels can vary drastically with diet and inflammatory status[7,28], suggesting that it should be possible to define specific scenarios that lead to nitrite accumulation in both host and environmental niches. Most parts of the human intestine are hypoxic and vary in pH level (from pH 5 to 8)[29], fulfilling two key variables in our proposed model of NapA-dependent fitness (Supplementary Fig. 15). When nitrate is present in the intestine, we speculate that enteropathogens could take advantage of these conditions to either maintain viability by nitrite-dependent growth arrest in acidic fermentative states or to support expansion in alkaline respiratory conditions (Supplementary Fig. 15). We propose that *V. cholerae* functionally integrates environmental cues including nitrate levels, O_2 concentration and pH to sustain a metabolic state conducive to optimal fitness. Interestingly, *napAB* expression is highly upregulated in stool samples from cholera patients[30], raising the possibility that Nap may also contribute to other steps in the pathogen's lifecycle, such as transmission between hosts and/or persistence/growth in the marine environment.

METHODS

Bacterial strains and growth conditions.

Vibrio cholerae El Tor C6706 (streptomycin-resistant $LacZ^+$ or $LacZ^-$ derivatives), *Escherichia coli* EHEC O157:H7, *E. coli* K12, *Citrobacter rodentium* DBS100 and *Salmonella typhimurium* ATCC 4028 strains were used in this study. Additionally, we constructed *Vibrio cholerae* C6706 Δ*napA* (Sm^r), and Δ*napA adhE* (Sm^r) mutant strains. Where appropriate, antibiotics were added to *V. cholerae* and *E. coli* cultures at the following concentrations: 200 (streptomycin, Sm), 100 (carbenicillin, Cb) and 50μg/mL (kanamycin, Km). Strains were grown aerobically at 37ºC in 15 ml tubes containing 3 ml LB medium (10 g tryptone, 10 g NaCl, and 5 g yeast extract/L) shaking at 300 rpm. To generate anaerobic growth curves, 1.5×10^7 aerobically grown cells were inoculated into 15 ml tubes containing 13 ml defined M9 minimal (1% glucose or an alternative carbon source elsewhere indicated) or buffered (50 mM phosphate buffer at the indicated pH) complete LB medium supplemented with or without KNO_3 and $NaNO_2$. Throughout the manuscript we use "-N" and "+N" to refer to cultures grown in the absence or presence of KNO_3, respectively. All growth curves in the manuscript depict growth under hypoxia. To establish hypoxic conditions, tubes were closed with rubber septa to ensure an airtight system. Oxygen was removed by sparging the headspace in each tube with argon gas for 3 minutes. DMSO, fumarate and TMAO were also used as alternative electron acceptors to nitrate at concentrations of 20 mM. Where specified, M9 minimal media cultures were supplemented with the indicated nutrients at the following concentrations: 10 mM (succinic, malic and formic acids) and 0.3mM (valine, glutamic acid and aspartic acids). The artificial mix of amino acids used in Supplementary Figure 7 was composed of 0.3 mM Ile/Leu/Trp/Asn/His/Val/Ser/Ala/Glu/Met/Thr. Casamino acids were supplemented at 1%. 10 mM sodium orthovanadate (Sigma), 20 mM itaconic acid (Sigma) and 40 μM antymonyl tartrate trihydrate (Sigma) were used as phosphofructokinase inhibitors.

Construction of plasmids and *V. cholerae* mutants.

V. cholerae mutants were created by allelic exchange with the suicide plasmid pCVD442[31]. To generate *napA, adhE, and napA adhE* deletion mutants, ca. 1 kb upstream and downstream DNA fragments flanking each gene were PCR-amplified with the primers listed in Table S2. Upstream and downstream fragments were spliced together by overlap PCR. The resulting ca. 2 Kb fragments were doubly digested with SacI/SalI and cloned into pCVD442 digested with the same enzymes. Plasmids were transformed into *E. coli* DH5α λpir for amplification. Constructs were confirmed by sequencing, transformed into the *E. coli* donor strain SM10 λpir and conjugated overnight at 37°C with *V. cholerae* C6706 by mixing equal volumes (1.5 ml) of exponential phase cultures, concentrating into 50 μl, and spot-plating. Single crossover *V. cholerae* were selected on LB plates with Sm and Cb. Re-streaked single colonies were then plated on salt-free LB agar containing 10% (w/v) sucrose and Sm. Colonies were streaked on Cb plates to confirm loss of pCVD442 and then checked by PCR for successful deletion mutants.

The plasmid pET28b was used for N-terminal His-tagged protein overexpression and nickel affinity purification. Open reading frames encoding the *V. cholerae* phosphofructokinase

(PFK) (VC2689) were PCR-amplified, digested and cloned into the pET28b NdeI/EcoRI sites. Plasmids were transformed into *E. coli* DH5α for amplification. Constructs were confirmed by sequencing and transformed into the *E. coli* BL21 prior to PFK purification.

Assessment of nitrate and nitrite reduction in *V. cholerae* and other enteric bacteria.

Strains were grown in M9 minimal medium + 1% glucose containing either 1 mM of KNO_3 or $NaNO_2$. After 24 hours, the plates were centrifuged at 8000g for 3 minutes and supernatants transferred to a new tube. To quantify the anoxic NO_3^- and NO_2^- reduction capacity of each strain, the final concentration of NO_2^- in the medium was determined with a spectrophotometric assay[32]. Equal volumes of sulfanilamide (58 mM, Sigma) and *N*-(1-Naphthyl) ethylenediamine (772 μM, Sigma) were added and NO_2^- concentration was quantitated by measuring resulting absorbance at 540 nm and comparing to a standard curve of $NaNO_2$ alone.

Light microscopy and viability determination of *V. cholerae* cultures.

V. cholerae cells were immobilized on 1% LB agarose pads. Phase contrast microscopy was performed using a Zeiss Axio Imager Z2 microscope (Zeiss, Germany) equipped with a Plan-Apochromat 63X phase contrast objective lens and an ORCA-Flash 4.0 LT digital CMOS camera (Hamamatsu Photonics, Japan). Image analysis and processing were performed with Zen2 software. To quantify viable cells in the hypoxic cultures, we used the Live/Dead BacLight Viability Kit (Thermo Fisher), following the manufacturer's instructions. To investigate the integrity of the genetic content of *V. cholerae*, 2ml of cells from anoxic cultures were centrifuged and resuspended in 100μl of PBS buffer, then incubated for 5 min with Hoechst 33342 (Sigma) 0.1 mg/mL. Hoechst-positive cells were identified by fluorescence microscopy. Cell viability at 24 hours incubation was also quantified with a Biorad S3e cell sorter at an excitation wavelength of 488 nm and an emission wavelength of 525/30 nm (for green) or 655 nm (for red). Genomic DNA (gDNA) was isolated from 48-hour hypoxic culture with GE Healthcare Life Science kit and gDNA integrity was analysed by agarose (1 %) gel electrophoresis.

Quantification of secreted organic acids.

Secreted organic acids from *V. cholerae* cultures grown under anoxic conditions were analysed by ultra-performance liquid chromatography (UPLC). To avoid metabolic leakage[32] from damaged cells, samples were incubated for 24 h instead of 48 h in the indicated conditions. 1 ml from each culture was centrifuged at 8,000 g for 5 minutes, and the supernatant was filtered through a 0.22 μm filter. 0.5μl of the filtered supernatant were separated by UPLC using a BEH C18 column (130 Å, 1.7 μm, 2.1 mm by 150 mm; Waters, USA). Absorbance was monitored at 204 nm. Elution conditions were: flow rate 0.125 ml min^{-1}; temperature 30 °C; 7 min isocratic elution in 10 mM H_2SO_4. Identification and quantification of the different organic acids was performed by comparison to standards of known concentration and peak integration. Samples were analysed in triplicate.

Metabolomic analysis of anaerobically growing *V. cholerae*.

V. cholerae cells were incubated with or without 3 mM of NO_3^- or 1.5 mM NO_2^- in oxygen-purged minimal M9 medium as previously described. After 24 hours, cells were collected by centrifugation at 8000g for 15 minutes at 4ºC and washed twice with phosphate-buffered saline (PBS). The pellet was frozen with liquid nitrogen and stored at −80 ºC. The metabolite extraction protocol, instrument settings, data processing, and quality control have been described in detail previously[33–36]. In brief, 900 μL of extraction buffer (90/10 v/v methanol:water) including internal standards were added to 100 μL of sample material. The sample was shaken at 30 Hz for 3 minutes in a mixer mill and proteins were precipitated at +4 °C on ice. The sample was centrifuged for 10 minutes at 8,000 g and +4 °C. 200 μL of supernatant were transferred to a micro-vial and solvents were evaporated. 30μL methoxyamine in pyridine (15 μg/μL) was added to each GC vial, and the resultant mixture was vigorously vortexed for 10 min. The solution was vortexed again for 10 min following of addition of N-Methyl-N-(trimethylsilyl) trifluoroacetamide (MSTFA) with 1% thrimethylchlorosilane (TMCS) as catalyst. GCMS analysis was performed as described previously[33,34]. For data evaluation, all non-processed MS-files from the metabolic analysis were exported from the ChromaTOF software in NetCDF format to MATLAB™ R2011b (Mathworks, Natick, MA, USA), where all data pre-treatment procedures, such as base-line correction, chromatogram alignment, data compression and Hierarchical Multivariate Curve Resolution (H-MCR), were performed using custom scripts[35]. The extracted mass spectra were identified by comparisons of their retention index and mass spectra with libraries of known retention time indices and mass spectra[36]. All multivariate statistical investigations (PCA, OPLS-DA) were performed using the software package SIMCA version 13.0.2 (Umetrics, Umeå, Sweden). Metabolite concentrations were normalized to the protein levels of each sample by the Bradford assay (Bio-Rad Laboratories).

pH-dependent viability assays.

To study the effect of the pH on *V. cholerae* viability under anoxic conditions, two types of experiments were performed: *V. cholerae* viability analysis after 48 hours in **(i)** pre-conditioned medium (PCM), and **(ii)** in fresh M9 culture medium adjusted to pH 5.7, 6.2 or 7, with HCl or with acetic, formic and lactic acids. For (i), *V. cholerae* was hypoxically grown for 48 hours in the presence or absence of 3 mM NO_3^- in M9 + 1% glucose. Supernatants from these cultures were harvested at 8,000 g for 15 minutes, filtered and then used as the pre-conditioned media (PCM) from -N or +N conditions. PCM samples that were kept at the original pH (5.7 for -N and 6.2 for +N) or adjusted to the opposite pH (6.2 or 5.7) were inoculated with 1.5×10^8 CFU *V. cholerae* for 48 hours under hypoxic conditions. A ten-fold dilution series of cells was plated for each condition at 48 hours onto LB agar to determine viability. For (ii), to exclude the effect of glucose fermentation on extracellular pH we used M9 + 10mM succinate (a non-fermentable carbon source). *V. cholerae* from M9 succinate media pH-adjusted with HCl or various organic acids were serially plated on LB agar to determine viability after 24 hours of growth at 37ºC. Samples were analysed in triplicate.

Screening of a defined transposon mutant library for NO_2^- toxicity.

A defined transposon insertion library in *V. cholerae* strain C6706[37] was used to screen for strains that, in contrast to the wild-type strain, are able to couple nitrate reduction with growth in minimal M9 medium. *V. cholerae* C6706 wild type and mutant strains were grown in 200 µl of LB in 96-well plates under aerobic conditions at 37ºC for 24 hours and used to inoculate 96-well plates containing 200 µL minimal M9 medium with or without 20 mM NO_3^-. The 96-well plates were sealed with aluminium films to avoid oxygen transfer and incubated without agitation for 24 hours at 37ºC. Differential growth was analysed by measuring final absorbance at 600 nm in the 96-well plates.

Determination of *in vitro* and *in vivo* nitrate reductase (NR) activity.

V. cholerae C6706 was grown aerobically in LB medium for 24 hours. 1.5×10^7 cells from those cultures were grown hypoxically in buffered complete LB medium at pH 6 and pH 8 in the presence of 20 mM of NO_3^-. These cultures were collected by centrifugation at 8,000 g for 5 min at 4°C and washed four times with 50 mM Tris/HCl buffer (pH 7.5) to remove the NO_2^- produced during Nap induction. Whole cells were using to preserve Nap complex integrity. Specific activities were calculated in nmol NO_2^- produced x min^{-1} x $mg.prot^{-1}$. The experiment were repeated three times and representative results are shown. The reaction mixture for methyl viologen-dependent NR contained 50 mM Tris/HCl buffer (pH 7.5), 20 mM KNO_3, 1.4 mM of methyl viologen and 5 µl of cell suspension (1–3 µg of protein). For determination of succinate-dependent NR activity, the reaction mixture contained 50 mM Tris/HCl buffer (pH 7.5), 20 mM KNO_3, 20 mM of sodium succinate and 20 µl of cell suspension (20–60 µg of protein). For methyl viologen-dependent NR, the reaction was started by the addition of 50 µl of freshly prepared sodium dithionite solution (8 mg ml^{-1} in milliQ water). After incubation for 5 min (*in vitro* NR) or 30 min (*in vivo* NR) at 37°C, the reaction was stopped by vigorous shaking until the samples had lost their blue colour. NR activities were measured relative to the amount of NO_2^- accumulated from NO_3^- reduction. NO_2^- concentration was estimated after diazotization by adding the sulfanilamide/ naphthylethylene diamine dihydrochloride reagent[38].

Purification of recombinant PFK and BsrV.

V. cholerae PFK and BsrV enzymes were overproduced in *E. coli* strain BL21 as 6×His-tagged constructs from a pET28b vector. Overnight cultures of overexpression strains were diluted into 250 mL LB broth and grown until $OD_{600} = 0.5$. Flasks were supplemented with 1 mM IPTG and shaking at 37º C for 2 h. Cells were pelleted, and resuspended in equilibration buffer (Tris 50 mM, pH 7.5, 50 mM NaCl, with protease inhibitor cocktail (Roche)) and disrupted by passaging once through a French press. Lysates were centrifuged for 1 h (25,000 rpm, Beckman Coulter Avanti J26-XP centrifuge, JL-25.50 rotor) at 4°C. Nickel-NTA resin (0.5 ml resuspended in equilibration buffer) was then added to the supernatant, followed by incubation at 4°C in a rotating wheel. The lysate was separated from the resin by centrifugation for 1 minute at 3,220 g and the resin washed (5×10 ml) with washing buffer (equilibration buffer adjusted to 1 M NaCl) and eluted with 2ml of washing buffer containing 500mM imidazole. Fractions were subjected to SDS-PAGE and Coomassie

Brilliant Blue staining for purity assessment. Protein concentration was quantified with a Bradford assay.

Phosphofructokinase and BsrV *in vitro* enzymatic assays.

The PFK activity assay was performed in accordance with manufacturer's instructions (MAK093; Sigma-Aldrich) with purified *V. cholerae* PFK. This assay quantifies PFK activity by measuring its capacity to convert fructose-6-phosphate to fructose 1,6-diphosphate. This reaction produces ADP, which is converted to AMP and NADH by the reaction mix. The resulting NADH reduces a probe resulting in a colorimetric (450 nm) product proportional to the PFK activity of the sample. Specific activity was calculated in pmol NADH/mg protein. Racemase activity assays using purified BsrV protein were performed essentially as described in ref. [39] (see Extended Data Fig. 7 for schematic representation of both activities). To assess the effect of nitrite under low pH on PFK and BsrV activities, 5 μg of each enzyme were incubated for 4 hours in 50mM Tris HCl at pH 6 in the presence or absence of 20 mM sodium nitrite, and an aliquot of 0.1 μg protein collected and added into each specific activity reaction mix.

Measurement of membrane potential.

Membrane potential was measured by flow cytometry using the BacLight bacterial membrane potential kit (Invitrogen). 1mL aliquots from each culture were pelleted, washed once and resuspended in 600 μl PBS and incubated with 30 μM 3,3'-diethyloxacarbocyanine iodide (DiOC2). As a control, to depolarize the membrane, instead of DiOC2, we added 5 μM carbonyl cyanide 3- chlorophenylhydrazone (CCCP). Samples were incubated for 15 min at 20 ºC in the dark. Fluorescence was measured with a Biorad S3e cell sorter at an excitation wavelength of 488 nm and an emission wavelength of 525/30 nm (for green) or 655 nm (for red).

Competition assays.

Aerobic overnight cultures of *V. cholerae* C6706 wild type *lacZ*$^+$ and *napA lacZ*$^-$ strains were harvested and 1×10^7 cells were co-inoculated at 1:1 ratio in 15 ml tubes containing 13 ml of M9 minimal medium or complete LB medium buffered at pH 6 or pH 8, with or without NO_3^- as specified. Tubes were closed with rubber septa and the oxygen was removed. After 8 hours of incubation under hypoxic conditions at 37°C, an aliquot was diluted and plated in LB agar plates containing X-Gal to enumerate WT and Δ*napA* bacteria in the culture. To obtain 24-hour CFU ratios, an aliquot from the 8 hour incubation culture was used to re-inoculate fresh LB tubes for additional 16 hours (24 hours in total). The same approach was followed to study the competitive capacity of *V. cholerae* C6706 wild type *lacZ*$^+$ against *E. coli* K12. Assays were performed in triplicate. Competitive index (CI) was determined by dividing the ratio of white (*V. cholerae* Δ*napA* mutant or *E. coli* K12 wild-type strains) to blue (wild-type *V. cholerae*) colonies by the ratio in the inoculum.

Streptomycin-treated adult mouse model of *V. cholerae* intestinal colonization.

The Sm-treated mouse model was performed similarly to previous reports[19,40,41]. 8-week-old male C57BL/6 were purchased from a commercial vendor (Charles River) and fasted for

4 hours before oral gavage with 100 μL of 200 mg/ml Sm. Mice were then given regular chow and water containing 5mg/mL Sm. After 72 hours, mice were orally gavaged with 100 μL of a 1:1 mixture of WT and Δ*napA V. cholerae* (approximately 2 ×10^9 total CFU per mouse) in 2.5% Na_2CO_3. Mice were sacrificed 24 hours post gavage and intestinal tissues were collected and homogenized by bead beating. All mouse work was performed according to a protocol approved by the Brigham and Women's Hospital IACUC (2016N000416). Sample sizes were chosen based on previous studies employing the same model[41, 21]. Mice were randomly divided into cages of 5 and cages were randomly selected to receive either a WT/lacZ or lacZ/napA inoculum. To prevent transmission between groups, we inoculated all animals in one cage with the same inoculum. Investigators were not blinded to the composition of the inoculum for each cage. Bacterial loads were quantified by plating on LB + Sm/X-gal and incubation overnight at 30 °C followed by blue/white colony counting. CI was determined by dividing the ratio of white (mutant) to blue (WT) colonies by the ratio in the inoculum.

Statistics and reproducibility.

Statistical significance was assessed with the Student's t-test or a Mann-Whitney U test where indicated. A p-value of less than 0.05 was considered statistically significant. Assays were performed with three biological replicates unless otherwise indicated. SD, standard deviation; SE, standard error of the mean.

Data availability.

Raw metabolomic data from *V. cholerae* samples grown anaerobically in the presence or absence of nitrate and nitrite have been appended.

Supplementary Material

Refer to Web version on PubMed Central for supplementary material.

Acknowledgments.

This work was supported by the Knut and Alice Wallenberg Foundation (KAW), The Laboratory of Molecular Infection Medicine Sweden (MIMS), the Swedish Research Council and the Kempe Foundation. The Waldor lab is supported by the Howard Hughes Medical Institute (HHMI) and the National Institutes of Health (NIH R01-AI-O42347). BS was supported by the National Sciences and Engineering Research Council of Canada (NSERC PSGD3–487259). We thank Cedric Patthey for help with the cell sorting experiments, and John J. Mekalanos for the *V. cholerae* C6706 Tn-mutant library.

References.

1. Wallace N, Zani A, Abrams E & Sun Y The Impact of Oxygen on Bacterial Enteric Pathogens. Adv Appl Microbiol 95, 179–204, doi:10.1016/bs.aambs.2016.04.002 (2016). [PubMed: 27261784]
2. Vazquez-Torres A & Baumler AJ Nitrate, nitrite and nitric oxide reductases: from the last universal common ancestor to modern bacterial pathogens. Curr Opin Microbiol 29, 1–8 (2016). [PubMed: 26426528]
3. Arkenberg A, Runkel S, Richardson DJ & Rowley G The production and detoxification of a potent cytotoxin, nitric oxide, by pathogenic enteric bacteria. Biochem Soc Trans 39, 1876–1879 (2011). [PubMed: 22103543]

4. Braun M & Thony-Meyer L Cytochrome c maturation and the physiological role of c-type cytochromes in Vibrio cholerae. J Bacteriol 187, 5996–6004 (2005). [PubMed: 16109941]
5. Lopez CA, Rivera-Chavez F, Byndloss MX & Baumler AJ The Periplasmic Nitrate Reductase NapABC Supports Luminal Growth of Salmonella enterica Serovar Typhimurium during Colitis. Infection and Immunity 83, 3470–3478 (2015). [PubMed: 26099579]
6. Spees AM et al. Streptomycin-induced inflammation enhances Escherichia coli gut colonization through nitrate respiration. mBio 4, doi:10.1128/mBio.00430-13 (2013).
7. Winter SE et al. Host-derived nitrate boosts growth of E. coli in the inflamed gut. Science 339, 708–711 (2013). [PubMed: 23393266]
8. Bueno E, Mesa S, Bedmar EJ, Richardson DJ & Delgado MJ Bacterial adaptation of respiration from oxic to microoxic and anoxic conditions: redox control. Antioxid Redox Signal 16, 819–852 (2012). [PubMed: 22098259]
9. Winter SE et al. Gut inflammation provides a respiratory electron acceptor for Salmonella. Nature 467, 426–429 (2010). [PubMed: 20864996]
10. Cole J Nitrate reduction to ammonia by enteric bacteria: redundancy, or a strategy for survival during oxygen starvation? FEMS Microbiol Lett 136, 1–11 (1996). [PubMed: 8919448]
11. Heidelberg JF et al. DNA sequence of both chromosomes of the cholera pathogen Vibrio cholerae. Nature 406 (2000).
12. Almeida JS, Julio SM, Reis MA & Carrondo MJ Nitrite inhibition of denitrification by Pseudomonas fluorescens. Biotechnol Bioeng 46, 194–201 (1995). [PubMed: 18623304]
13. Fang FC Antimicrobial reactive oxygen and nitrogen species: concepts and controversies. *Nature reviews*. Microbiology 2, 820–832 (2004). [PubMed: 15378046]
14. Gao SH et al. Determining Multiple Responses of Pseudomonas aeruginosa PAO1 to an Antimicrobial Agent, Free Nitrous Acid. *Environmental science & technology* 50, 5305–5312 (2016). [PubMed: 27116299]
15. Yarbrough JM, Rake JB & Eagon RG Bacterial inhibitory effects of nitrite: inhibition of active transport, but not of group translocation, and of intracellular enzymes. Applied and environmental microbiology 39, 831–834 (1980). [PubMed: 6769392]
16. Zhou Y, Pijuan M, Zeng RJ & Yuan Z Free nitrous acid inhibition on nitrous oxide reduction by a denitrifying-enhanced biological phosphorus removal sludge. *Environmental science &* Technology 42, 8260–8265 (2008).
17. Lidder S & Webb AJ Vascular effects of dietary nitrate (as found in green leafy vegetables and beetroot) via the nitrate-nitrite-nitric oxide pathway. Br J Clin Pharmacol 75, 677–696 (2013). [PubMed: 22882425]
18. Tannenbaum SR, Fett D, Young VR, Land PD & Bruce WR Nitrite and nitrate are formed by endogenous synthesis in the human intestine. Science 200, 1487–1489 (1978). [PubMed: 663630]
19. Mandlik A et al. RNA-Seq-based monitoring of infection-linked changes in Vibrio cholerae gene expression. Cell Host Microbe 10, 165–174 (2011). [PubMed: 21843873]
20. Cameron DE, Urbach JM & Mekalanos JJ A defined transposon mutant library and its use in identifying motility genes in Vibrio cholerae. Proceedings of the National Academy of Sciences of the United States of America 105, 8736–8741 (2008). [PubMed: 18574146]
21. Nygren E, Li BL, Holmgren J & Attridge SR Establishment of an adult mouse model for direct evaluation of the efficacy of vaccines against Vibrio cholerae. Infection and Immunity 77, 3475–3484 (2009). [PubMed: 19470748]
22. Bergaust L, Mao Y, Bakken LR & Frostegard A Denitrification response patterns during the transition to anoxic respiration and posttranscriptional effects of suboptimal pH on nitrous [corrected] oxide reductase in Paracoccus denitrificans. Applied and Environmental Microbiology 76, 6387–6396 (2010). [PubMed: 20709842]
23. Bueno E, Bedmar EJ, Richardson DJ & Delgado MJ Role of Bradyrhizobium japonicum cytochrome c550 in nitrite and nitrate respiration. FEMS Microbiol Lett 279, 188–194 (2008). [PubMed: 18179591]
24. Rowley G et al. Resolving the contributions of the membrane-bound and periplasmic nitrate reductase systems to nitric oxide and nitrous oxide production in Salmonella enterica serovar Typhimurium. Biochem J 441, 755–762 (2012). [PubMed: 22039967]

25. Kelso HLBS, V. R; Laughlin RJ Effects of Carbon Substrates on Nitrite Accumulation in Freshwater Sediments. Applied and Environmental Microbiology 65, 5 (1999).
26. Philips SLJH; Verstraete W Origin, causes and effects of increased nitrite concentrations in aquatic environments. Reviews in Environmental Science and Biotechnology 1, 26 (2002).
27. Zakem EJ et al. Ecological control of nitrite in the upper ocean. Nature Communications 9, 1206 (2018).
28. Silvester KR,Bingham SA,Pollock JR,Cummings JH,O'Neill IK Effect of meat and resistant starch on fecal excretion of apparent N-nitroso compounds and ammonia from the human large bowel. Nutr Cancer 29,13–23 (1997) [PubMed: 9383779]
29. Fallingborg J Intraluminal pH of the human gastrointestinal tract. Danish Medical Bulletin 46, 183–196 (1999). [PubMed: 10421978]
30. Merrell DS et al. Host-induced epidemic spread of the cholera bacterium. Nature 417, 642–645 (2002). [PubMed: 12050664]
31. Donnenberg MS & Kaper JB Construction of an eae deletion mutant of enteropathogenic Escherichia coli by using a positive-selection suicide vector. Infection and Immunity 59, 4310–4317 (1991). [PubMed: 1937792]
32. Hawver LA, Giulietti JM, Baleja JD & Ng WL Quorum Sensing Coordinates Cooperative Expression of Pyruvate Metabolism Genes To Maintain a Sustainable Environment for Population Stability. mBio 7, e01863–16 (2016). [PubMed: 27923919]
33. J. A et al. Extraction and GC/MS analysis of the human blood plasma metabolome. Analytical Chemistry 77, 8086–8094 (2005). [PubMed: 16351159]
34. Gullberg J, Jonsson P, Nordstrom A, Sjostrom M & Moritz T Design of experiments: an efficient strategy to identify factors influencing extraction and derivatization of Arabidopsis thaliana samples in metabolomic studies with gas chromatography/mass spectrometry. Analytical Biochemistry 331, 283–295 (2004). [PubMed: 15265734]
35. Jonsson P et al. High-throughput data analysis for detecting and identifying differences between samples in GC/MS-based metabolomic analyses. Analytical Chemistry 77, 5635–5642 (2005). [PubMed: 16131076]
36. Schauer N et al. GC-MS libraries for the rapid identification of metabolites in complex biological samples. FEBS Letters 579, 1332–1337 (2005). [PubMed: 15733837]
37. Cameron DE, Urbach JM & Mekalanos JJ A defined transposon mutant library and its use in identifying motility genes in Vibrio cholerae. Proc. Natl. Acad. Sci. USA 105, 8736–8741 (2008). [PubMed: 18574146]
38. Nicholas DJD, and Nason A Determination ofnitrate and nitrite. Meth Enzymol 3, 981–984 (1957)
39. Espaillat et al. Structural basis for the broad specificity of a new family of amino-acid racemases. Acta Crystallographic Section D Biological Crystallography. 2014 70, 79–90. [PubMed: 24419381]
40. McDonald ND, Lubin JB, Chowdhury N & Boyd EF Host-Derived Sialic Acids Are an Important Nutrient Source Required for Optimal Bacterial Fitness In Vivo. mBio 7, e02237–02215 (2016). [PubMed: 27073099]
41. Sasabe J et al. Interplay between microbial d-amino acids and host d-amino acid oxidase modifies murine mucosal defence and gut microbiota. Nature Microbiology 1, 16125 (2016).

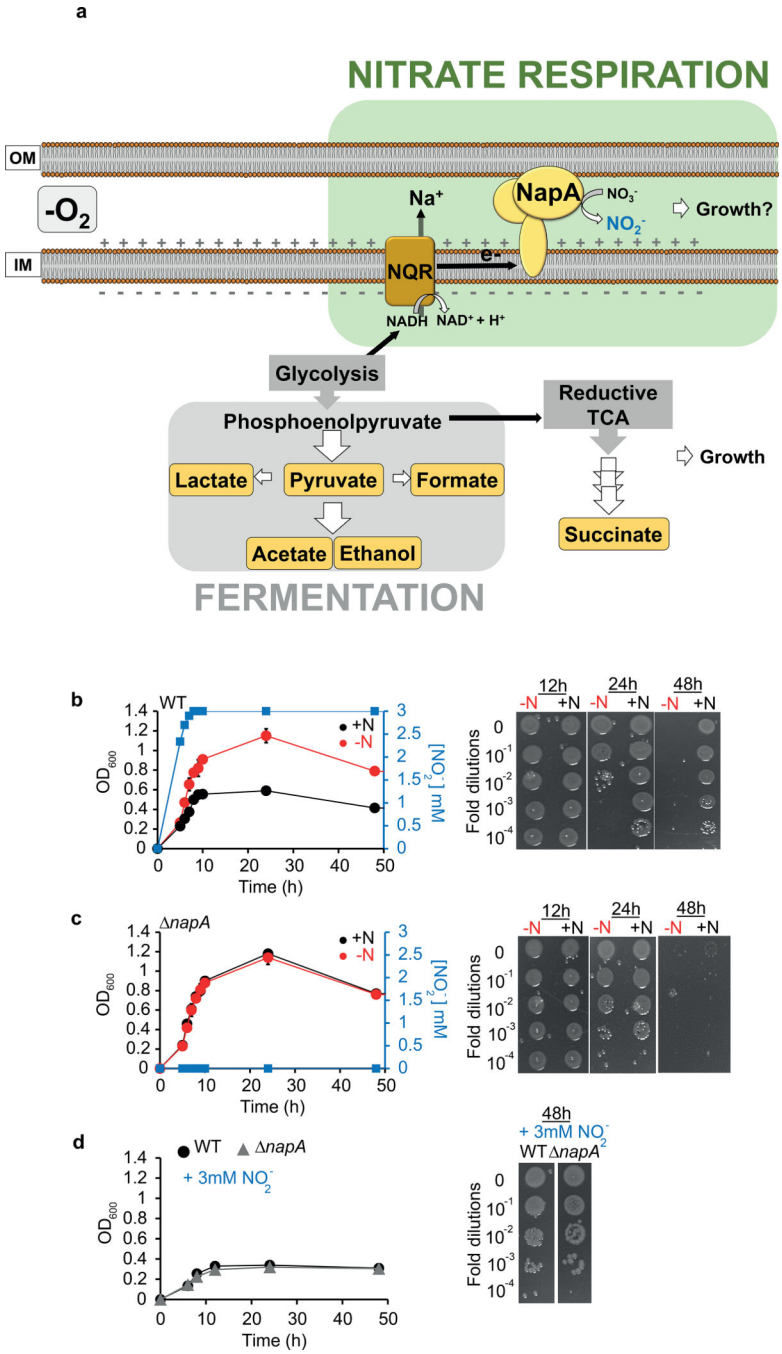

Figure 1 | . NO_2^- accumulation preserves*V. cholerae* viability at the cost of population expansion during anaerobic growth.

(a) Schematic of nitrate utilization in *V. cholerae.* In the absence of respiratory electron acceptors such as O_2 or NO_3^-, *V. cholerae* undergoes mixed-acid fermentation. Nap, nitrate reductase; NQR, Na(+)-translocating NADH:quinone oxidoreductase. **(b and c)** Optical density (OD_{600}) (left) and viability test (right) of **(b)** WT and **(c)** *ΔnapA V. cholerae* strains hypoxically grown in M9 minimal medium + 1% glucose in the absence (–N, red) or presence of 3mM NO_3^- (+N, black) or **(d)** both WT and *ΔnapA* in the presence of 3mM

NO_2^-. NO_2^- accumulation is shown in blue. Data are the mean of 3 biological replicates +/− SE. For viability tests, 3 independent replicates were analyzed with similar results.

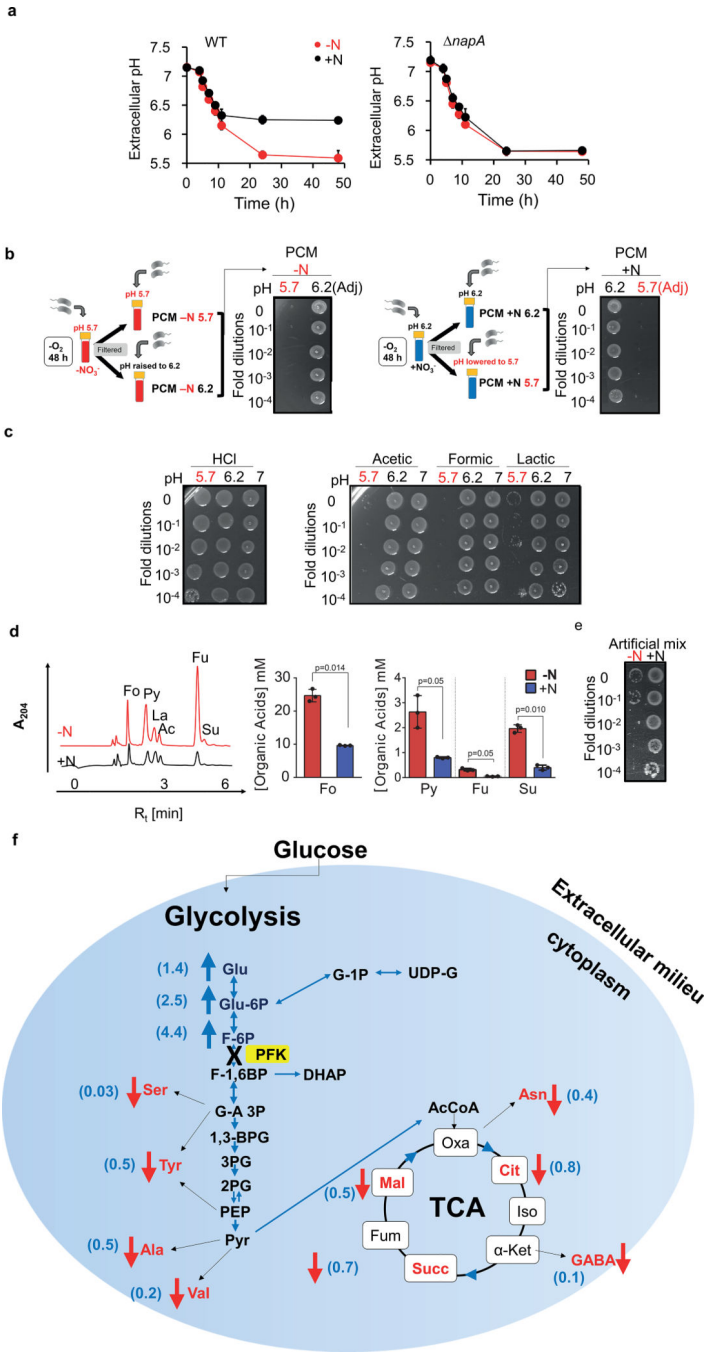

Figure 2 | . NO_2^- production during anaerobic growth slows toxic fermentative acidification of *V. cholerae*.

(a) Extracellular pH in cultures from Figure 1b. **(b)** Viability of WT *V. cholerae* to pre-conditioned media (PCM) from primary -N or +N hypoxic cultures at either the original pH or with the pH artificially adjusted (Adj) to 5.7 (killing pH in red) or 6.2. **(c)** CFU of WT *V. cholerae* after 48 hours of anaerobic growth in pH-controlled non-fermentable media. The agent used to control the pH is indicated. **(d)** UPLC analysis (left) and concentration (right) of organic acids in culture supernatants from 24-hours hypoxic -N (red) or +N (black) WT

cultures. Fo: formic, Py: pyruvic, La: lactic, Fu: fumaric, Su: succinic acids, respectively. **(e)** CFU of WT *V. cholerae* exposed to an exogenous mix of organic acids at concentrations determined in Panel d**. (f)** Comparative targeted metabolomics of *V. cholerae* hypoxic cultures with or without NO_2^- supplementation. Relative abundance indicated in parentheses. Data from **a, d, f** are the mean of 3 biological replicates +/− SE. Three independent replicates were analyzed in parallel in **b**, **c** and **e** with similar results. Pairwise comparisons were performed in **d** using two-tailed unpaired Student's t-tests.

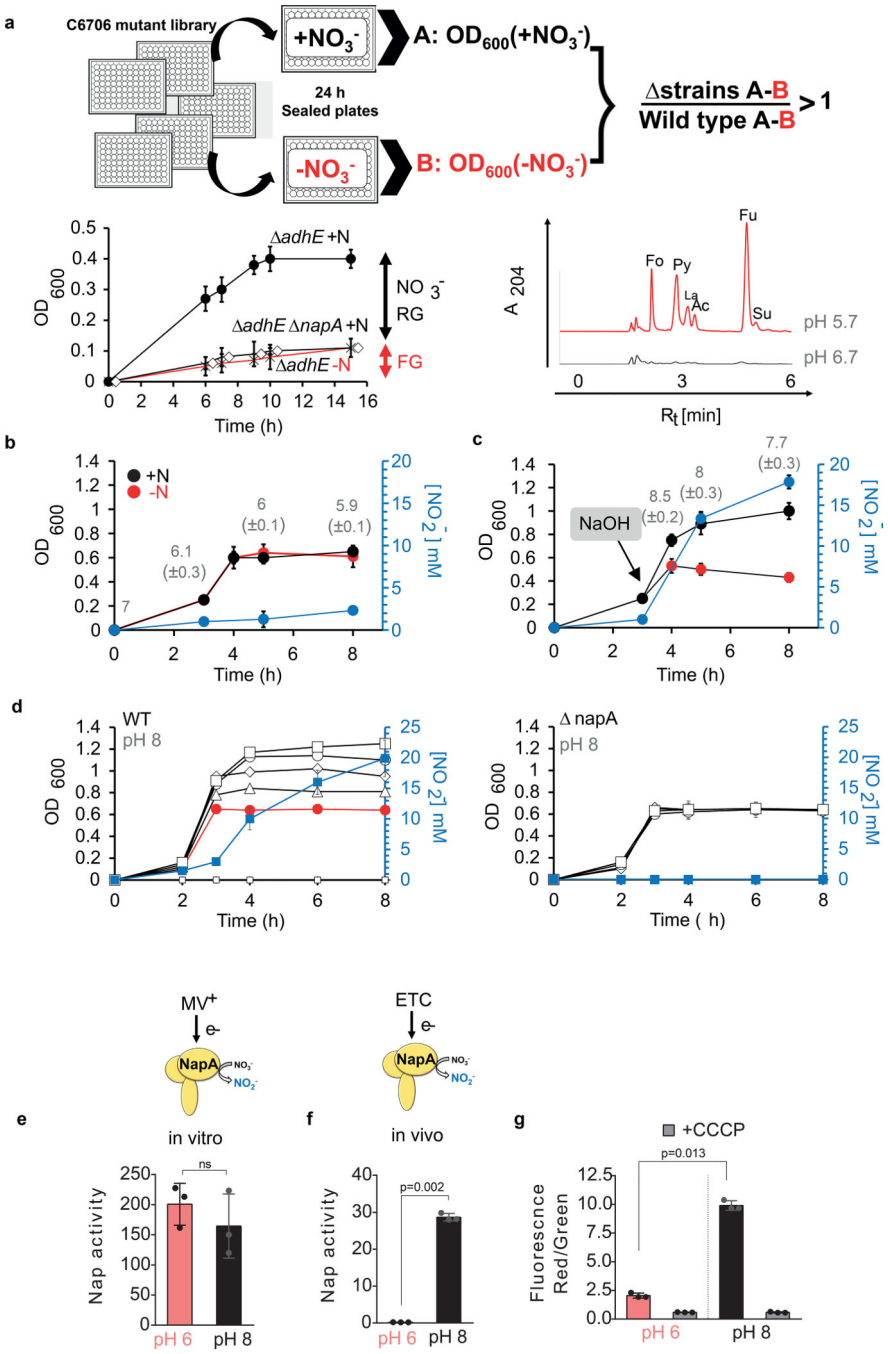

Figure 3 | . *V. cholerae* undergoes anaerobic NO_3^- respiration under alkaline conditions.

(a) Top: Screen to identify *V. cholerae* mutants insensitive to NO_2^--dependent growth arrest. Bottom: Analysis of the *ΔadhE* mutant selected from the screen. NO_3^- RG: nitrate respiratory growth; FG: fermentative growth. **(b)** Growth curves of WT *V. cholerae* in unbuffered LB in the absence (red circles) or the presence of 20 mM NO_3^- (black circles). NO_2^- accumulation and extracellular pH are indicated in blue and grey, respectively. **(c)** Same as Panel b but with added NaOH at 3 hours post-inoculation. **(d)** Dose-dependent effects of supplemented NO_3^- on WT or *ΔnapA V. cholerae* in LB buffered at pH 8. NO_3^-

was added at the following concentrations: 0 (red circles), 3 (open triangles), 5 (open diamonds), 10 (open circle) and 20 mM (open squares). **(e)** Methyl viologen (MV^+)-dependent nitrate reductase (Nap) (*in vitro*) activity (nmol NO_2^- produced/min/mg protein). **(f)** succinate-dependent Nap activity (*in vivo*). ETC, electron transport chain. **(g)** Membrane potential analysis from $DiOC_2$ staining and flow cytometry. Data are the mean of 3 biological replicates +/− SE. Pairwise comparisons (e, f, g) were made using two-tailed unpaired Student's t-tests. ns, not significant.

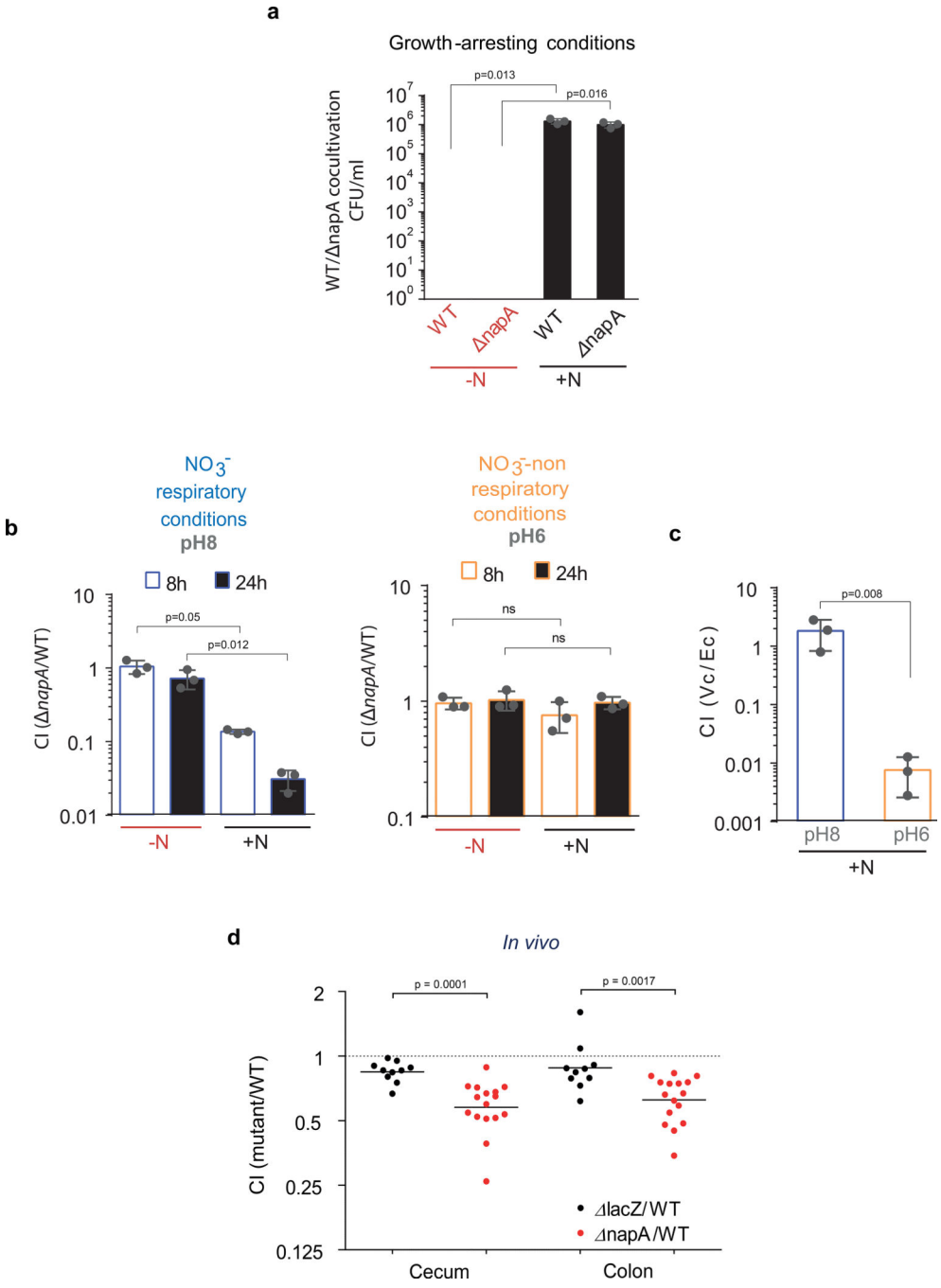

Figure 4. Disruption of NO_3^- respiration in *V. cholerae* negatively impacts fitness.

(a) CFUs of WT and *ΔnapA V. cholerae* co-cultures during anaerobic growth in M9 + 1% glucose with or without NO_3^- 3 mM after 48 hours of incubation. **(b)** *In vitro* competitive indices (CI) of WT *V. cholerae* vs the *ΔnapA* mutant during anaerobic growth in pH 8-buffered (NO_3^- respiratory conditions, pH 8) or non-buffered LB medium (NO_3^- non-respiratory conditions, pH 6) with or without supplemented NO_3^-. **(c)** *In vitro* competition of WT *V. cholerae* (Vc) against *E. coli* K12 (Ec) in identical conditions to panel b (see colour code). **(d)** *In vivo* competition of WT and *ΔnapA V. cholerae* in the streptomycin-treated

adult mouse colonization model. Data shown are CI values at 24 hours post colonization. A *ΔlacZ* (neutral) strain was used as a negative control to provide a baseline for statistical comparison. Data in panels a, b and c are the mean of 3 biological replicates +/− SE. Pairwise comparisons (a-c) were made using two-tailed unpaired Student's t-tests. Data in panel **d** is given as the geometric mean of all mice in each group (across 4 independent infections) +/− the geometric standard deviation.